International Research Journal of Multidisciplinary Scope(IRJMS), 2024; 5(4):784-797

IRJMS

Original Article | ISSN (O): 2582-631X DOI: 10.47857/irjms.2024.v05i04.01401

Compact Six Band Slot Antenna with Defective Ground Structure and E Shaped Strips for Bandwidth Enhancement in Wireless Applications

Kiran Hilal Sonawane*, Pravin Sahebrao Patil

Department of Electronics and Telecommunication, SSVPS BS Deore College of Engineering, Dhule, Maharashtra, India. *Corresponding Author's Email: khsona2009@gmail.com

Abstract

This article presents a novel approach for six-band operations and a comprehensive frequency range for wireless applications. The novel antenna has rectangular slot of small size 48x18mm^2 and has a T-shaped microstrip feed patch, a short-inverted T-shaped stub, two E-shaped stubs and two small square ground plane slots arranged on FR4 substrate with h= 0.8mm, a dielectric constant =3.5 mm and a loss tangent =0.004. Multiband and wide frequency responses in an antenna was achieved by etching E shaped stubs, inverted T-shaped stubs and rectangular slot in a defective ground plane. Radiating area and total size of antenna are smaller than three band antennas discussed in results section. Six-band slot antenna, resonance at 1.39 GHz (Global Position System-L3 band (GPS)), 3.36 GHz (Worldwide Interoperability for Microwave Access (Wi-MAX)), 5.26GHz (IEEE 802.11a (Wireless Local Area Network) WLAN)), 5.96 GHz (Vehicle to Vehicle Communications (V2V)), 7.27 GHz (C-band for Military Communications) and 8.41GHz (X-band for Satellite Communications) frequency bands. Six band rectangular slot antenna is investigated and designed using IE3D software. To verify simulation results, an antenna is fabricated and tested. The antenna exhibit S11<-10 dB bandwidth of 8.57% (1.34-1.46 GHz), 7.97% (3.25-3.52 GHz), 6.85% (5.07-5.43 GHz), 2.54% (5.82-5.97 GHz), 3.84% (7.14-7.42 GHz), 4.83 %(8.27-8.68GHz). The closed contact between measured and simulated results supports effectiveness of suggested approach.

Keywords: Defective Ground Structure, Global Positioning System, Vehicle to Vehicle Communication, Wireless Local Area Network.

Introduction

Since 5G connectivity has just been adopted in India, the demand is in terms of bandwidth enhancement without modifications to existing antennas. Different types of bandwidth enhancement techniques are used for different applications. One of today's most analytical subfields in communication systems is wireless technology (1). Microstrip antennas have gained popularity in various applications, and their thin, planar profile makes them well-suited for integration into modern communication devices. For several decades, the micro-strip antenna has gained widespread recognition as the most promising alternative for wireless applications (2). An antenna is a device used as a transceiver. Therefore, the speed of transmitting and receiving signals presents a challenge, particularly gives accelerated pace of advancement of communication systems both fixed and portable requires the switch to high data rates to cover a larger region due to the growth in network users. Therefore, high bandwidth (BW) is needed to cover all wireless services, including mobile devices. Wideband and ultra-wideband (UWB) low-profile antennas can be used to simplify design and reduce production costs (3). An increasing number of contemporary communication devices uses slot antennas, as of their enticing qualities, which include being very affordable, having a small footprint, and being lightweight. The coexistence of numerous communication systems and the ability of multiband slot antennas, to combine various bands into a single antenna have attracted a lot of attention in these areas. Filtering and duplexing antennas support increasing the system's frequency selectivity by removing the antenna and filter network's mismatches and losses (4). Multiband antennas are also advantageous for achieving best wireless quality and a variety of applications on one device.

(Received 23rd June 2024; Accepted 22nd October 2024; Published 30th October 2024)

Multiband antennas indeed offer advantages when it comes to reconfiguration and integration with switching and control circuits (5). Thus, designing an antenna with more than one operating band is attractive and has been researched in academic and industry. The antenna's effectiveness is quite low, ranging from 70% for simulation to 50% for measurement stated by Sun (6). Several multiband antennas have been studied for the desired antenna such as Planer inverted F antenna (7). A lot of compact MPA designs make use of defective ground structures (DGSs). DGSs have a range of shapes, from basic forms like spiral, V, U, H and I shapes (8) to more complex ones such as intricate ones like split-ring resonators (SRR) (9) and dumbell-shaped. Lightweight antennas are even more necessary in radio communication technologies, like WLAN, GPS and WiMAX. Several multiband antennas have been studied for the desired antenna. For MIMO applications (10, 11) and three antennas resonating in the 2.4, 5.2, and 5.8 GHz bands. A wide bandwidth and a small form factor are essential for constructing multiband antennas that can be combined with other devices such as varactor diode having limitation in terms of power handling capability (12). By engraving many slots with numerous stubs in ground planes, such as multiband monopole slot antenna (13), open ended slot antenna (14), dual band using twin T-stub (15), arc strip (16), D-shaped (17), periodic slot antenna (18) and so on. The design of a small multifrequency slot antenna (19), a triple-slot antenna with single tunes and multiple tune frequencies (20), a compact tri-band slot antenna (21, 22), a compact UWB printed slot antenna (23), an annual ring slot antenna (24), a compact three triangle shaped DGS (25) and circular slot antenna (26) are discussed. The application of defective ground structures is consumed to increase the antenna's performance. A pattern etched on the ground plate of the antenna is used to control the scattered inductance and capacitance of DGSs. A Transmission lines with slow wave and band-gap characteristics are consequently produced in the study by Niu (27). In the study of Jeneath (28) state that multi resonance frequency switching was designed with three pin diodes in the ground plane which covers 1.33 to 8.7 GHz. In the study of Jayashri (29) proposed and studied two port CPW-fed MIMO antenna with wide bandwidth and high isolation for future wireless applications.

In this paper two major challenges are addressed (narrow operating band and multiband operations) by introducing a new design methodology for compact rectangular slot antenna without increasing the form factor. The multiband antennas are the smallest, least expensive, and offer the highest data rates. In the study Cao (30) the rectangular slot antenna reported is considered as reference in this presented work. In the study of Shalini (31) concentric ring and DGS is used for multiband operation. Multilayer technology (32) is used for bandwidth enhancement. This paper focuses on a rectangular slot etched in ground structure-as DGS based multiband antenna (with six resonant frequencies) and a comprehensive range for wireless applications. A multiband is constructed of a rectangular slot, two E-shaped stubs, inverted T-shaped stubs, folded T-shaped feed patch and defective ground structure to obtain a wide range of applications. Multiband operations are investigated (with six resonant frequencies) which were not reported by any of the authors discussed in literature survey. In methodology section the design process of rectangular slot antenna with dimensions are discussed. In result and discussion section, describes the simulation and measurement results with comparison followed with conclusions.

Methodology

Here, innovative design to create a six-band microstrip rectangular slot antenna for applications in GPS, Wi-MAX, WLAN, V2V, X-band, and IEEE-C-band satellite communications is presented. Microstrip patch antennas produce circular polarization and are used for WiMAX Applications. Circularly polarized antennas can resolve the problems caused due to transmitter-to-receiver coordination. The best six bands at approximately 1.39, 3.36, 5.26, 5.9, 7.27, and 8.41 GHz were generated. The proposed filtering antenna has an inverted T shaped stub, one E-shaped stub and another mirror E shape stub, a T shaped micro-strip feed patch, two symmetrical square ground plane slots on either side, and a rectangular ground plane slot. In our suggested design, a single radiating element creates a special frequency band. The harmonics of a T shaped patch in our concept resulted in two frequency bands. A defective ground plane's rectangular slot allows surface current to be altered, producing two

additional resonances in addition to the two harmonic resonant frequencies produced by folding the top section of the T-shaped feed patch twice. Proper impedance matching also helps in improving the bandwidth of antenna because impedance matching circuits add some additional resonances.

Rectangular patch is designed using an equation [1].

$$W = \frac{\frac{V_o}{C}}{2f_r}\sqrt{\frac{2}{\epsilon_r + 1}} \quad [1]$$

Calculation of effective dielectric constant (ϵ_{reff}) using equation [2] given by

$$\epsilon_{reff} = \frac{\epsilon_r + 1}{2} + \frac{\epsilon_r - 1}{2}\left[1 + 12\frac{h}{W}\right]^{-\frac{1}{2}} \quad [2]$$

Calculation of effective length (L_{eff}), length extension and radiating length is found using equation [3], [4] and [5] as shown below

$$L_{eff} = \frac{\frac{V_o}{C}}{2f_r\sqrt{\epsilon_{reff}}} \quad [3]$$

Calculation of length extension (ΔL)

$$\frac{\Delta L}{h} = 0.412\frac{\epsilon_{reff} + 0.3\left(\frac{W}{h} + 0.264\right)}{\epsilon_{reff} - 0.258\left(\frac{W}{h} + 0.8\right)} \quad [4]$$

Calculation of radiating length

$$L = L_{eff} - 2\Delta L \quad [5]$$

Calculation of actual ground plane is done using equation [6] and [7].

Dimension of ground plane is six times greater than the dimension of patch

$$L_g = 6h + L \quad [6]$$

$$W_g = 6h + W \quad [7]$$

Where L = the length of radiating patch, W = width of radiating patch, h= height of FR4 substrate, ε_r = relative permittivity of substrate, ε_{eff} = effective relative permittivity of patch. The rectangular slot antenna has a rectangular ground plane and measures L1×W1=48×18mm², this plane was examined and set up as depicted in Figure1. Defective rectangular ground planes have dimensions of Ws and Ls which are 44mm and 56 mm, respectively. The radiating portion, with dimensions of 48 x 18mm² consists of four parts: two monopoles of E-curved stubs are positioned over the rectangular slot, one on the left and another on the right, with an inverted T-curved stub inside the rectangular slot. The higher ends are folded on both sides to create a tiny form factor for the inverted T stub. Using the microstrip feed technique, the substrate is positioned with a rectangular slot on top of substrate and an inverted T stub on top rectangular slot with feed patch on another side. To match impedance the impedance distribution should be minimum and maximum at the edges of patch. So at the end the patch having step and double folded as shown in Figure1. The impedance is 50 ohms when a feed patch with a 1.76 mm width is utilized. To achieve compression, as shown in Figure1, the upper part of the feed patch is doubled, and both sides are folded. For desired impedance matching, a step is added to nearer center of T-shaped microstrip feed patch.

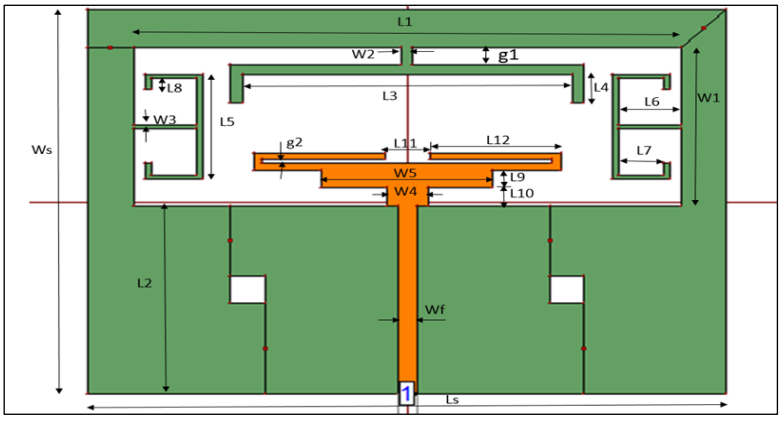

Figure 1: Geometry of Rectangular Slot Antenna

A rectangular slot antenna produces six resonant conditions with frequencies of approximately 1.41024, 3.36346, 5.24827, 5.92038, 7.28504 and 8.44795 GHz, corresponding to bands 1, 2, 3, 4, 5 and 6. One E-shape and another mirror E-shape curved stubs for WiMAX applications produce a second band @3.3 GHz. The Band-1 @1.41024 GHz is created for GPS service using a rectangular slot and an inverted T-shaped stub. To support WLAN applications, band 3 is generated at a resonant frequency of 5.24827 GHz by T-shaped microstrip powered patches and inverted-T stubs. Band 4

which is applicable for V2V applications is introduced by the T-shaped quarter wavelength feed patch at 5.92038 GHz. The FR-4 substrate has a dielectric constant of 3.5, a height of top surface of 0.8 mm, and loss tangent of 0.004. On either side of the feed patch, two 3 x 3 mm long square-shaped additional slots are introduced as modification in ground plane as display in Figure 1. Table 1 correspond to final design of proposed antenna. Other strip line circuits are mounted on the PCB, and the feed line is positioned in the middle of a ground plane. Figure 2 shows simulation result of path antenna for reflection coefficient. The placement of the feed line is symmetrical for comparison purpose. Figure 1 show the design of a slotted antenna as well as its top and bottom dimensions.

Table 1: Dimensions of Rectangular Slot Antenna

L1	**L2**	**L3**	**L4**	**L5**	**L6**	**L7**	**L8**
48.0	21.52	29	3.32	11.90	5.57	4	1.37
L9	**L10**	**L11**	**L12**	**g1**	**g2**	**W1**	**W2**
1.95	1.95	3.95	11.5	2.1	0.47	18	0.725
W3	**W4**	**W5**	**Wf**	**Ws**	**hs**	**Ls**	
0.38	3.675	15	1.75	44	0.8	56	

Results and Discussion

The designed rectangular slot antenna contains multiple frequency bands and various radiation-related components. For each of the following four cases, an IE3D software computer simulation of S_{11} was used. (i) When just T-shaped power feed patch is present; (ii) when an inverted T-shaped stub and T-shaped power feed patch are present; (iii) when only two components are present the E-shaped with the T-shaped power patch is present and (iv) when the complete design emerges, finally conclude from modeling data that the slotted antenna generates the 1.4, 4.6, and 5.6 GHz frequency bands when condition (i) is met. Rectangular slots produce band 1 at 1.4 GHz, T-shaped power feed patches produce band 3 at 5.26827 GHz, and rectangular slots produce band 4 at 5.96038 GHz. Band 1 is displaced down in case (ii) Bands 3 and 4 share frequencies, when T and inverted T is used. Figure 1 illustrates entire fabricated geometry using E and mirror E curved stubs, an inverted T curved stub, and double folded T-shaped feed patch.

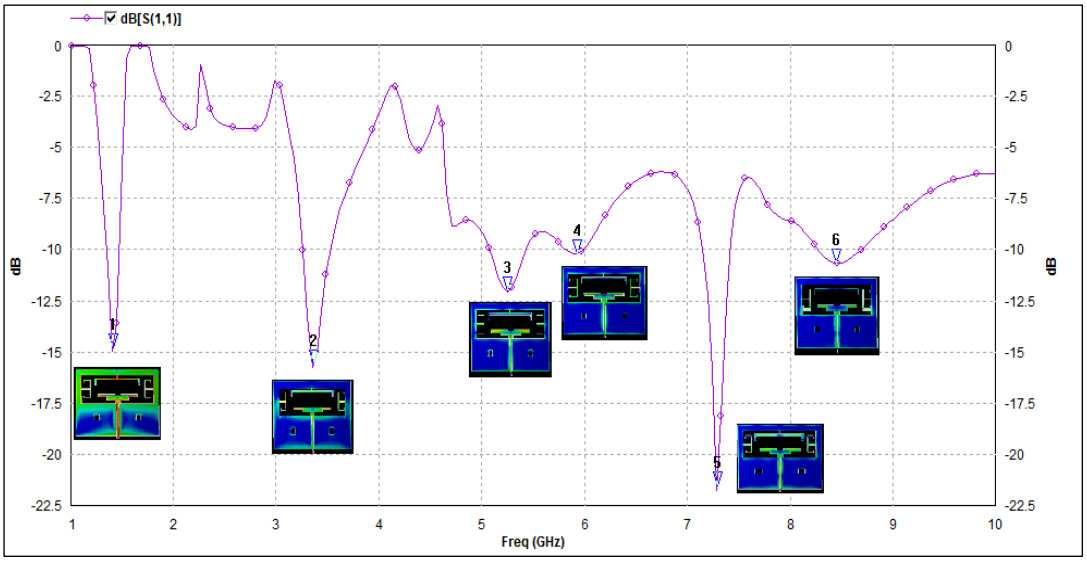

Figure 2: Simulation Result of Patch Antenna for S_{11}

Six resonant frequency bands are shown in Figure 2, with resonance frequencies of 1.4, 3.3, 5.2, 5.9, 7.2 and 8.4 GHz respectively. With a reflection coefficient of S_{11}<-10 dB, Figure 2 shows a slot antenna with six frequencies at 1.39765-1.46032 GHz for GPS systems (used in the L3-band), 3.25662-3.52709 GHz for WiMAX state, 5.07467-5.43152 GHz for IEEE 802.11a WLAN systems, 5.82-5.97 GHz for V2V communications, 7.14613-7.42979 GHz for satellite communications (C-band and X-band) and 8.27509-8.68462 GHz for X-band satellite communications. Figure 2 depicts the

simulation result for S_{11}. The numerous parameters, like L1, L3 to L10, W1, W5, and gl, can be changed to alter the frequency bands. To achieve the required outcomes, adjust the planned geometry for various purposes. A simulation is used to determine how the frequency range changes as a result of parameter changes. Here a ground plane with fixed dimensions are employed that remains constant when parameter values change. A scalar simulated surface current distribution at the edge of rectangular slot and at the feed point, which is flipped upside down (inverted T-shaped) stub operating @1.40 GHz for band 1. The inverted T stub current is closer to the surface plane on an inverted T curve. Using equation [8] one may determine the Band 1 resonant frequency which relates to dimensions of rectangular slot in ground plane. Theoretically, the slot dimension indeed to be used to define a resonant frequency (f1).

$$f_1 = \frac{c}{2(L_1 + W_1)\sqrt{\epsilon}} = 1.43GHz \qquad [8]$$

Where ϵ is dielectric constant of FR4 substrate

$$\epsilon \approx \frac{(\epsilon_r + 1)}{2} = 2.25 \qquad [9]$$

ϵ_r= relative permittivity of substrate
C = speed of light in free space
L1 = length of the rectangular slot
W1 = width of the rectangular slot

The resonant frequency declines, as the surface current distribution through the edge of the slot gl alters band 1 as well as the method of current flow. The two E-shaped monopoles are the focal points of the current, which give the resonant frequency and are given by equation [10] as

$$f_2 = \frac{c}{4\left(L6 + \frac{L5}{2} + L7 + L8\right).\sqrt{\epsilon}} = 2.98GHz \qquad [10]$$

Figure 1 shows that L6, L5, and L7, may be modified to retuned resonant frequency band 2, these dimensions are related to E shaped and mirror E shaped stubs. Figure 3 shows fabricated rectangular slot antenna showing bottom and top view. It is evident from Figure 4(B) that the flipped upside-down stub interferes with the simulated surface current distribution, which lowers the ideal condition at frequency of 3.36 GHz. At 5.2 GHz for band 3 as depicted in Figure 4(C), the frequency is jointly determined by the double fold extended stubs of the T-shaped power patch and flipped upside down stubs. Both the horizontally expanded T-shaped feed patch and the inverted T-shaped stub receive current, determines the resonance frequency. Figure 4(D) for band 4 at 5.9 GHz depicts the current flowing through a T-shaped power feed path that is parallel to that in Figure 4(C), but with a shorter wavelength. Figure 3 shows fabricated rectangular slot antenna shows bottom and top view.

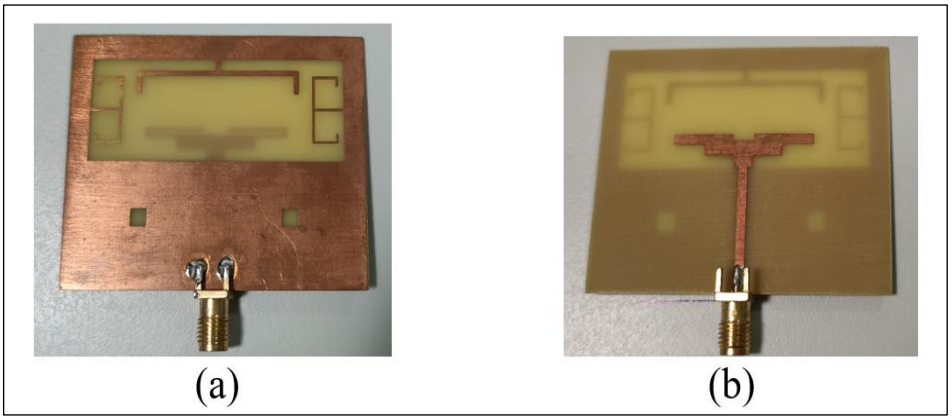

Figure 3: Photographs of Final Module (A) Bottom View, (B) Top View

Figure 3 shows a prototype antenna for measurement with a bottom and top view. The simulated surface current increases as a result of the bands produced by introducing two squares on the ground plane. For study purposes, simulated current distributions vs frequency are depicted in Figure 4. Electromagnetic energy that flows into or out of the patch via the feed probe combination. In the middle of the patch, there is no electric field; on one edge, it is maximal, and on the other, it reverses direction. The current (magnetic field) is maximum at the center of patch and minimum on the opposite sides of patch, while the voltage (electrical field) is zero in the center and maximum on one edge and reverses its direction (minimum) on opposite edge. Hence the distribution of

impedance is minimum at the center and maximum on both edge of patch (32). Surface current distributions are shown for frequencies of 1.41 GHz, 3.36 GHz, 5.24 GHz, 5.92 GHz, 7.28 GHz, and 8.44 GHz. Figures 4 shows the current distributions are different for all resonance conditions. At 1.41 GHz, the major current flows through a rectangular slot, an inverted T shaped and T shaped feed patch.

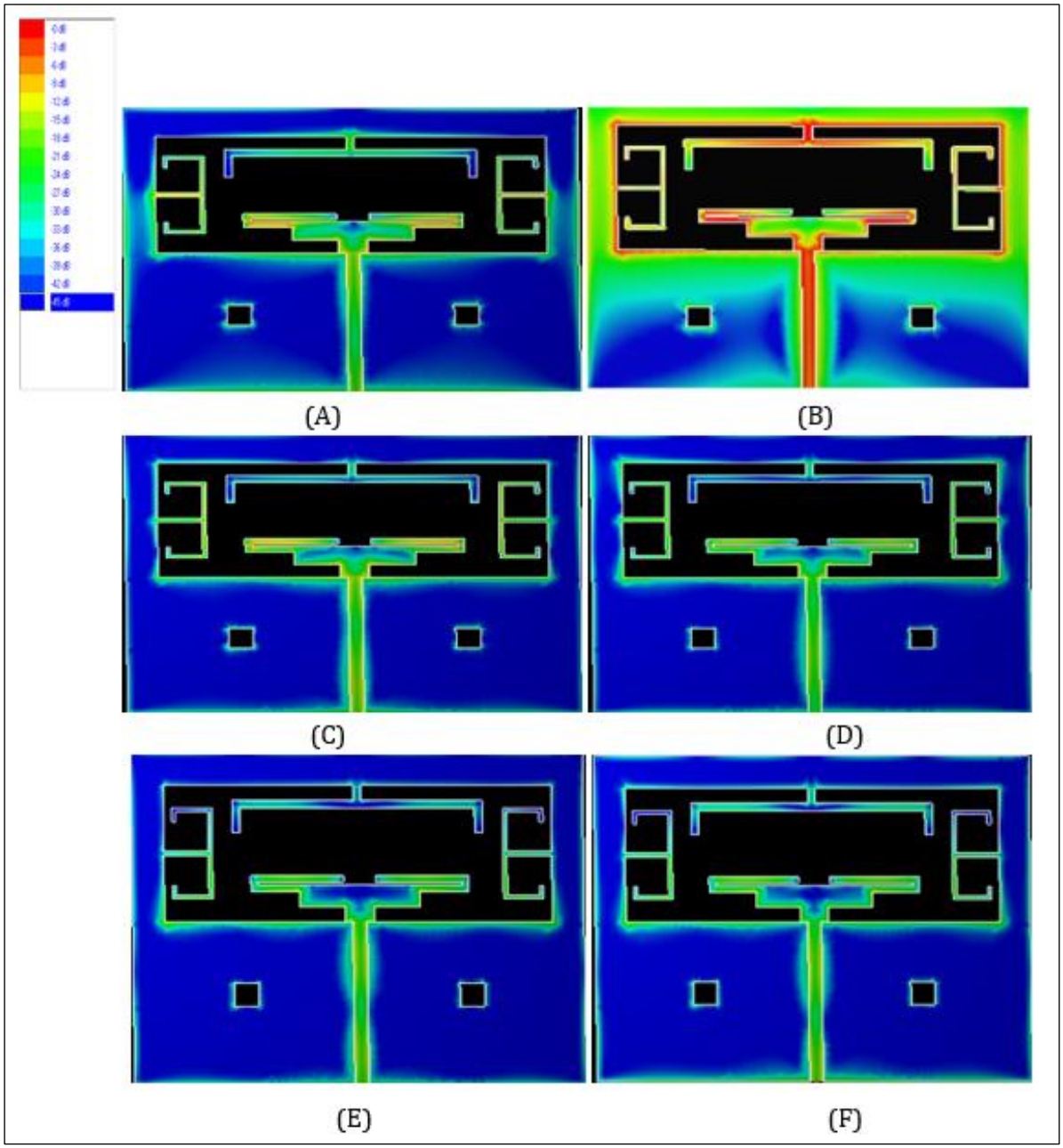

Figure 4: Surface Electric Field Distributions (A)1.41 Ghz, (B)3.36 Ghz, (C)5.24 Ghz, (D)5.92 Ghz, (E)7.28 Ghz, (F)8.44 Ghz

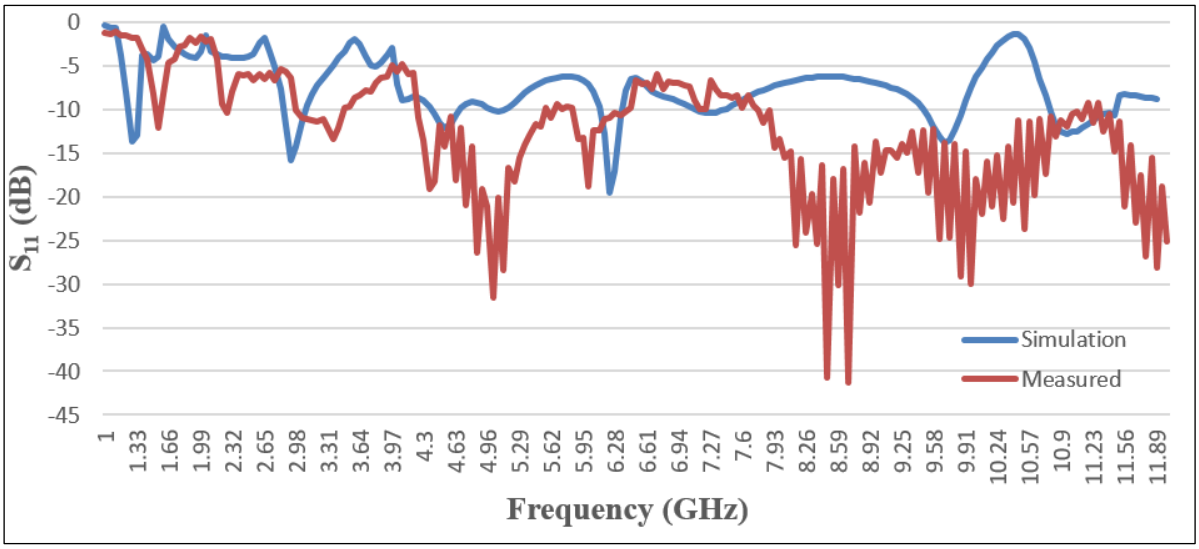

Figure 5: Simulated and Measured Reflection Coefficients

Table 2: Stimulation Results and Experimental Validation

Variable	Freq. (GHz)	S11	FL (GHz)	FH (GHz)	Bandwidth %	Bandwidth (MHz)
Simulation	1.39	-13.57	1.34	1.46	8.57	120
	3.36	-14.21	3.25	3.52	7.97	270
	5.26	-11.84	5.07	5.43	6.85	360
	5.96	-10.1	5.82	5.97	2.54	150
	7.27	-18	7.14	7.42	3.84	280
	8.41	-10.73	8.27	8.68	4.83	410
Measured	1.5	-12.12	1.5	1.58	5.19	80
	3.36	-13.42	2.98	3.42	13.75	440
	4.35	-31.52	4.24	5.41	24.24	1170
	6	-18.77	5.89	6.39	3.14	500
	8.48	-41.27	7.76	12	42.91	4240
	9.6	-29.95				

Using IE3D software, a computer simulation of the microstrip six band slot rectangular antenna is performed. The simulated S_{11} is shown in Figure 2. Six frequency bands were observed on the slotted antenna for S_{11}<-10 dB from 1.34 to 1.46 GHz, 120 MHz for GPS systems, 3.25-3.52 GHz for WiMAX, 5.07–5.43 GHz and 5.82–5.97 GHz for IEEE 802.11a WLAN systems and IEEE 802.11p V2V respectively, 7.14–7.42 GHz for the C and X satellite bands, and 8.27-8.68 GHz for X-band satellite communication. In the IE3D simulation, the coaxial cable is not taken considered. With the use of a vector network analysis tool, ROHDE and SCHWARZ, the prototype antenna is tested. The simulated and measured S_{11} are depicted in Figure 5. The S_{11} results at 1–10 GHz were measured by the subminiature version A (SMA) connector. The antenna is shown to have six frequency bands. For the GPS system (in L1 frequency band is 1563 to 1587 MHz), the measured frequency bands (for S_{11}@-10 dB) are 1.501–1.581 GHz (bandwidth: 80 MHz); during prototype testing resonant at 2.265 GHz at -10.48 dB; 2.98 to 3.42 GHz for WiMAX, 4.245 to 5.51 GHz for 802.11a WLAN, 5.895–6.39 GHz for 802.11p V2V communication; and 7.765–12 GHz for the C and X bands for satellite communications. Figure 5 displays the observed findings as the red line and the simulated results as the blue line.

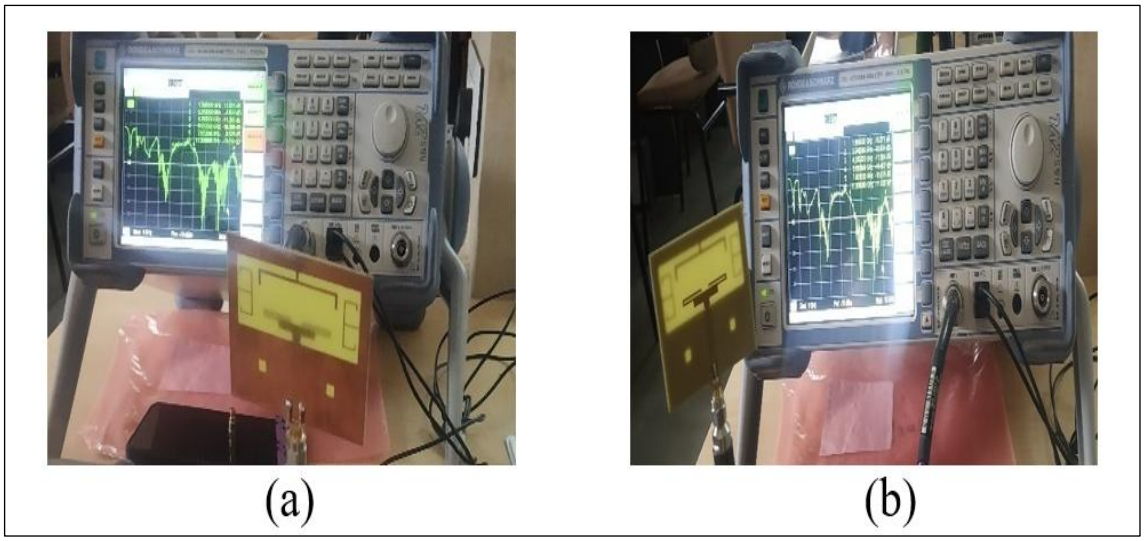

Figure 6: Measurement Setup (a) and (b) From 1 to 10 Ghz

Figure 6 depicts the microwave band measurement setup for S_{11}. Due to feeding cable, small difference between the measured and predicted outcomes. During simulation a cable was not used. During the measurement, a cable is used with the measured system (ROHDE and SCHWARZ system). At lower frequencies, ground plane becomes electrically thin, affecting the distribution of currents and potentially leading to undesired effects such as back radiation to feeding cable. The performance of simulation and measurement are quite similar. In measurement resonance occured at 1.5@-12.12 dB, 2.26 GHz@-10.48 dB, 2.98-3.42 GHz having a peak of -13.42 dB, 4.24-5.51 GHz having a maximum peak of -31.52 dB, 5.89-6.39 GHz having a peak of -18.77 dB, and 7.76-12 GHz having a peak of -41.27dB. The modeling and measurement findings show extremely high agreement in Figure 2 and 5. Table 2 shows simulation and measured results validation.

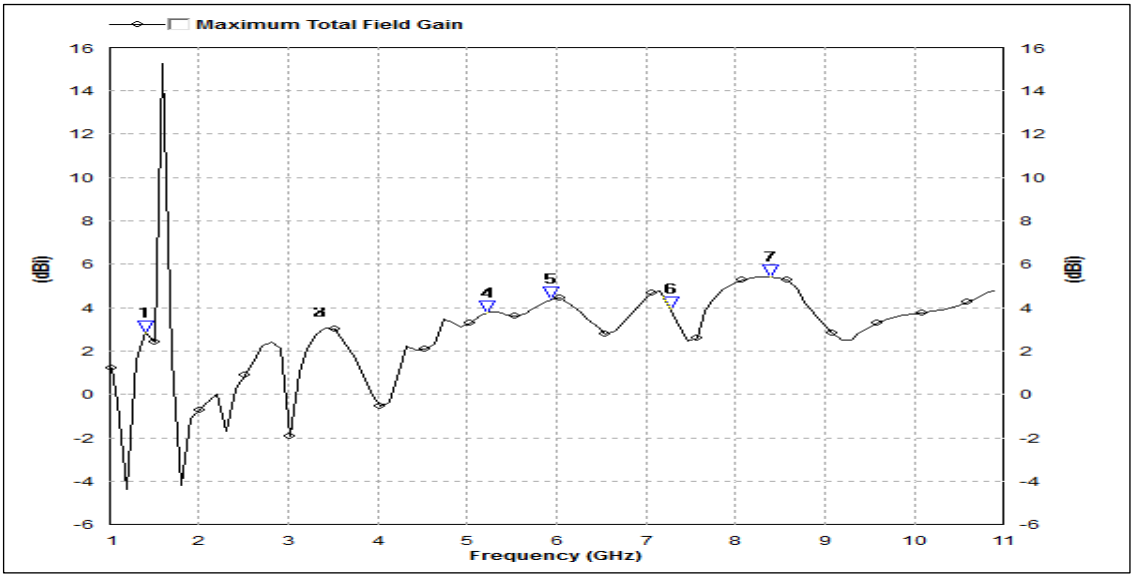

Figure 7: Simulated Total Field Gain

Figure 7 depicts the simulated gain for band 1, which is 2.82dBi. Band 2 has a gain of 2.88dBi, Band 3 has a gain of 2.88dBi, and Band 4 at 5.96 GHz has a gain of 3.76dBi. Band 5 has a gain of 4.38dBi, similarly band 6 has a gain of 3.93dBi. Figure 8 shows antenna efficiency mentioned in Table 3. Figure 9 shows radiation pattern in x-y and x-z mode for different resonant frequencies. Radiation pattern shows bidirectional and omnidirectional pattern in x-z and x-y field respectively.

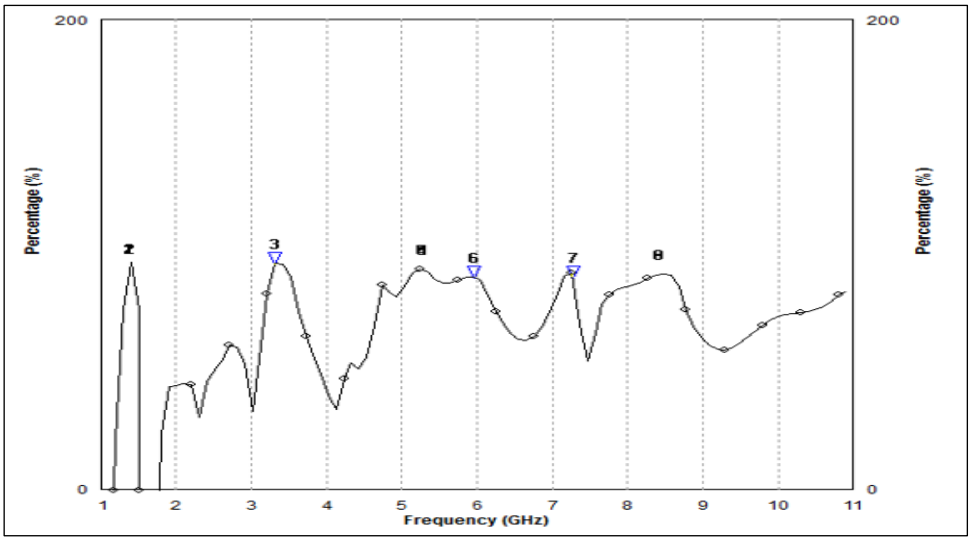

Figure 8: Antenna Efficiency

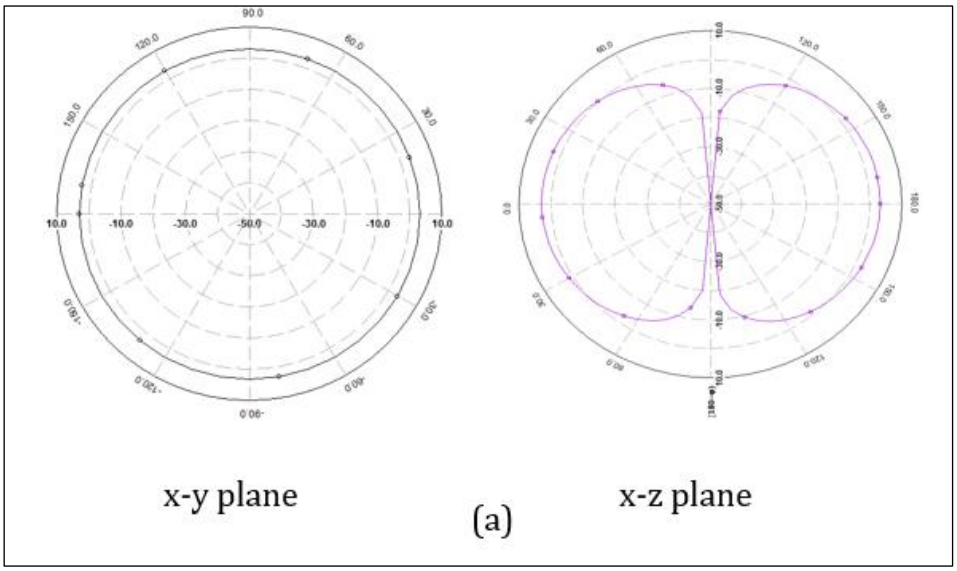

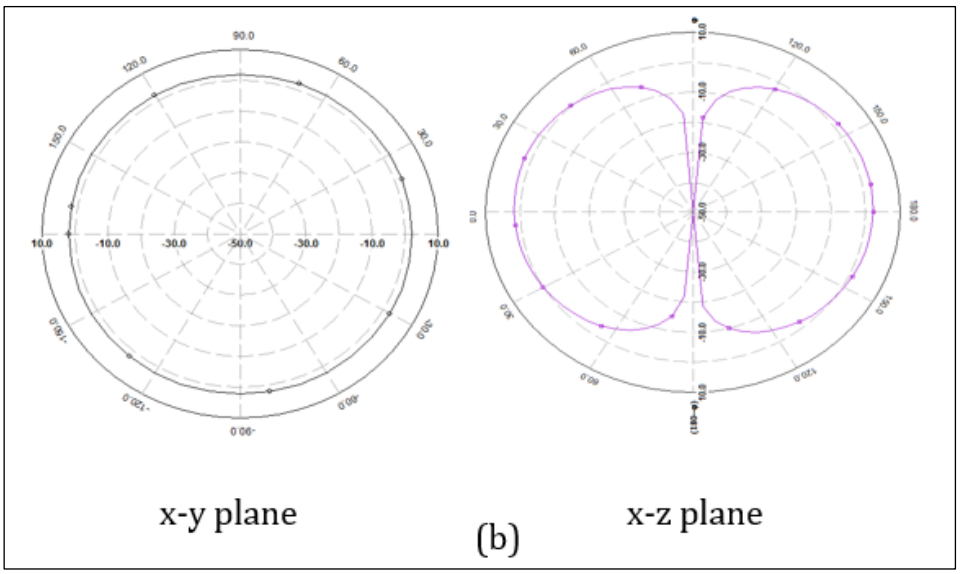

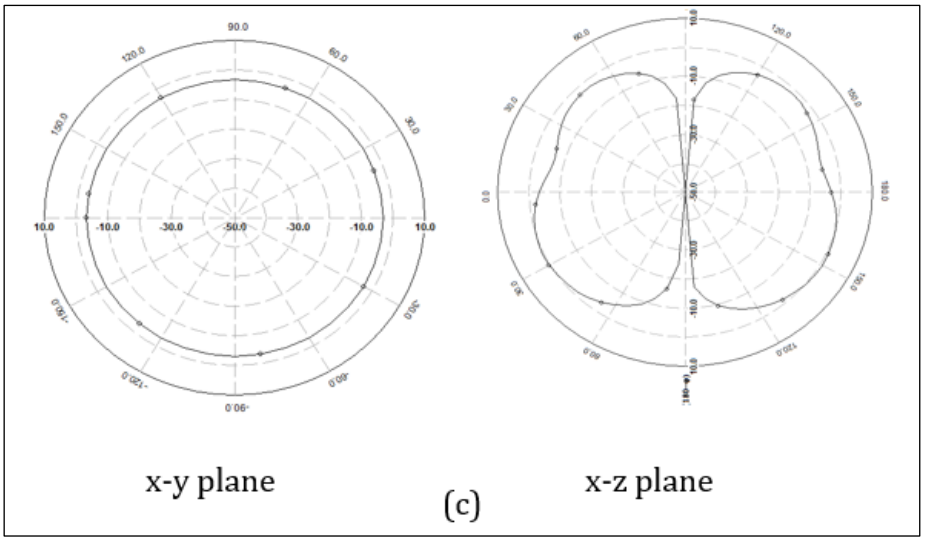

(c)

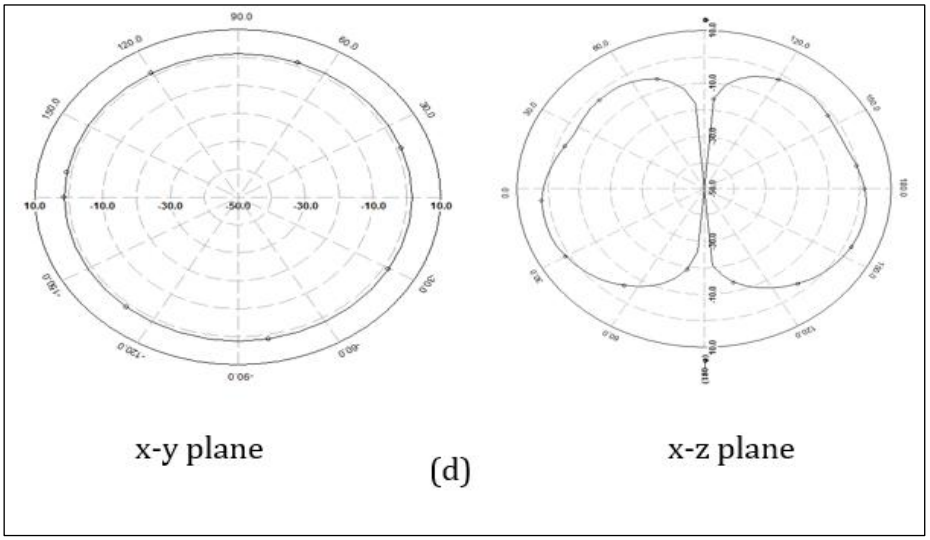

(d)

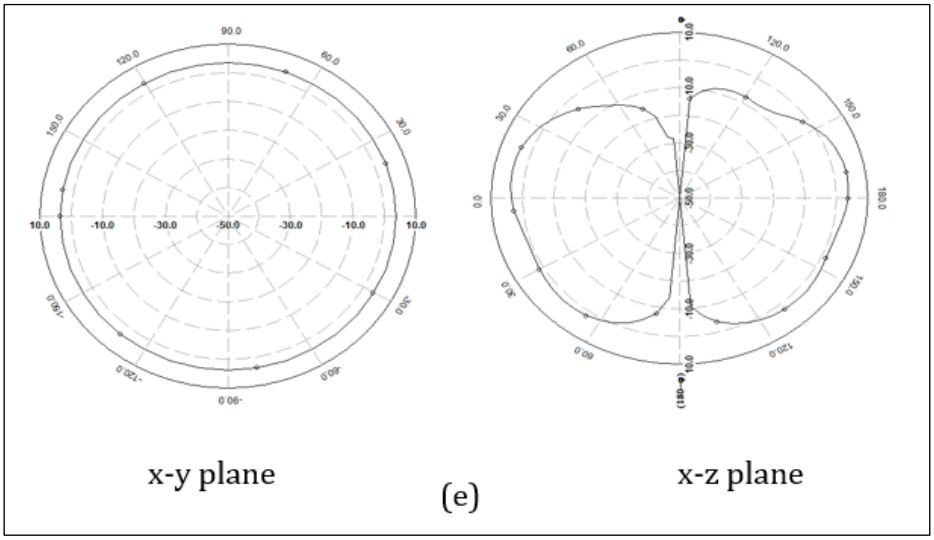

(e)

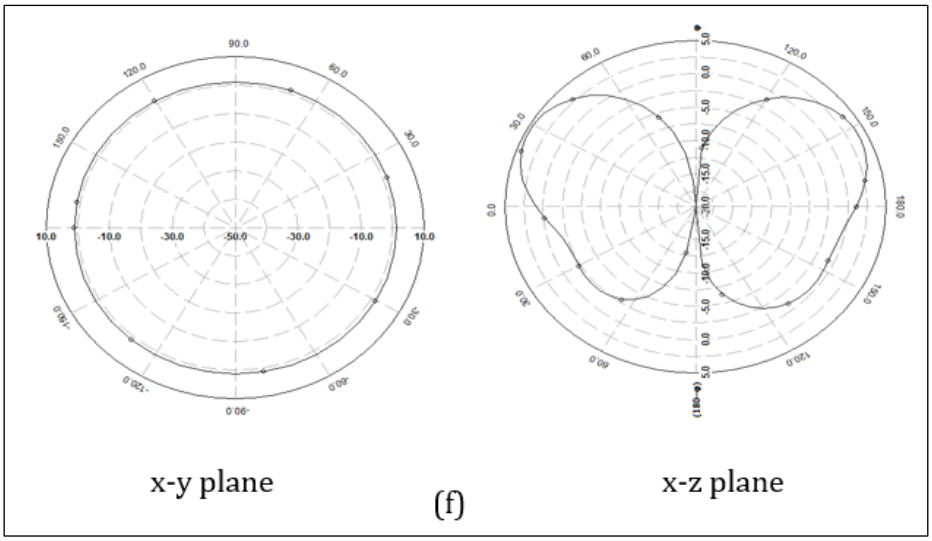

Figure 9: Computer-Simulated Radiation Pattern in x-y and x-z Plane (a) 1.39 GHz, (b) 3.36 GHz, (c) 5.26 GHz, (d) 5.96 GHz, (e) I 7.27 GHz and (f) 8.42 GHz

From Figure 9 we conclude that the radiation pattern in x-y plane are ominidirectional. In x-z plane the radiation pattern have a dumbbell shape. At low frequency the ground plane of antenna becomes electrically small and some currents will flow back form antenna to outer surface of feeding cable. This results in radiation inaccuracy and also alters the current distribution on antenna hence the return loss S_{11}. To improve the accuracy in measurement the feeding cable is covered with EM suppressant tubing to absorb unwanted radiation.

Table 3: Stimulation Results and Experimental Validation

Ref	Size (mm)	Gain (dBi)	Resonant Frequency (GHz)	No. of bands	Bandwidth %	Efficiency %	Approaches	Pattern
(19)	1.05 X 1.05	2.33	2.46	03	NA	NA	Sickle-shaped slots	Omnidirectional
		3.14	3.59		NA	NA		
		2.89	5.69		NA	NA		
(20)	0.46 X 0.85	3.0	2.6	03	19.6	88	C, open ended and L shaped slots	Omnidirectional
		4.3	3.5		20.7	95		
		5.2	5.5		14.5	97		
(21)	0.46 X 0.39	3.86	2.5	03	22.2	NA	Sickle-shaped slots	Omnidirectional
		3.52	3.5		12.3	NA		
		4.32	5.6		23.2	NA		
(22)	0.38 X 0.44	3.01	2.5	03	18.60	NA	Square slot with symmetrical L strip	Bidirectional
		3.02	3.5		24.93	NA		
		2.92	5.15		13.51	NA		

(23)	0.24 X 0.21	-6	2.45	03	4.50	NA	Octagonal-shaped slot and stepped rectangular patch	Omnidirectional
		NG	4.5		3.87	NA		
		2.5	6.5		4.30	NA		
(30)	0.44 X 0.35	3.55	1.57	04	5.6	76.8	Stepped rectangular patch	Bidirectional
		3.93	2.45		5.86	80.1		
		5.02	3.5		23	96.6		
This Work	0.44 X 0.35	4.86	5.2	06	13.7	85.5	Rectangular Ground Plane with E and inverted T stub	Omnidirectional
		2.82	1.39		5.19	93.92		
		2.88	3.36		13.75	96.01		
		2.88	5.26		24.24	93.50		
		3.76	5.96		8.14	90.14		
		4.38	7.27			90.14		
		3.93	8.42		42.91	91.23		

Gains of more than 2 dB are present at all frequencies of the proposed design, as shown in Table 3. This is because the reversed T curved patch and the E curved stub have the smallest possible gap between them. The gain also increases when distance increases. Table 3 shows performance comparison with different bandwidths, reflection coefficients, gains, strucuture and radiation pattern of rectangular slot antenna for different frequencies. Finally maximum bandwidth and gain obtained at 8.42 GHz with a return loss -10.73, which is good candidature for design.

Conclusion

The design of a multiband rectangular ground structure microstrip antenna for wireless communication is described. The defective ground plane is modified to obtain a wide bandwidth and multiband response. The multiband rectangular slot antenna with DGS is used for Future Wireless. The antenna dimensions are optimized to obtain performance at different resonance conditions. The proposed antenna is resonates at six frequencies to realize characteristic at over a wide frequency range from 1.34 to 8.68 GHz. The designed antenna can be obtained closer result in terms of the reflection coefficient and gain. Six frequency bands are obtained at about 1.39, 3.36, 5.26, 5.96, 7.27 and 8.42GHz which cover the GPS, WiMAX, WLAN, V2V, C band and X band satellite communication systems respectively.

Abbreviations

IEEE: Institute of Electrical and Electronics Engineers, MIMO: Multiple Input Multiple output, FR4: Flame Retardant 4, SRR: Split Ring Resonator.

Acknowledgement

The authors will want to acknowledge the enabling research environment provided by the college.

Author Contributions

Kiran Hilal Sonawane: Conceptualization, Methodology, Original Draft Preparation, Data Curation, Investigation, Reviewing, Editing, Formal Analysis, Visualization. Dr. Pravin Sahebrao Patil: Supervision, Project Administration, Funding Acquisition.

Conflicts of interest

The authors do not have any conflicts of interest.
Dr. Pravin Sahebrao Patil: Supervision, Project Administration, Funding Acquisition.

Ethics approval

Approved by the institutional review board.

Funding

No funding received for the research.

References

1. Mohammed AS, Kamal S, Ain MF, Ahmad ZA, Ullah U, Othman M, Hussin R, Ab Rahman MF. A review of microstrip patch antenna design at 28 GHz for 5G applications system. International Journal of Scientific and Technology Research. 2019; 8(10):341-352.
2. Kasabegoudar VG and Reddy P. A review of low profile single layer microstrip antennas. International Journal of Electrical and Electronic Engineering and Telecommunications. 2022; 11(2):122-131.
3. Saeidi T, Ismail I, Wen WP, Alhawari AR, Mohammadi A. Ultra-wideband antennas for wireless communication applications. International Journal of Antennas and Propagation. 2019;2019(1):7918765.
4. Xie Y, Chen FC, Qian JF. Design of integrated duplexing and multi-band filtering slot antennas. IEEE Access. 2020; 3(8):126119-126126.
5. Ali T, Khaleeq MM, Biradar RC. A multiband reconfigurable slot antenna for wireless applications. AEU-International Journal of Electronics and Communications. 2018;1(84):273-280.
6. Sun XL, Cheung SW, Yuk TI. Dual-band monopole antenna with frequency-tunable feature for WiMAX applications. IEEE Antennas and Wireless Propagation Letters. 2013; 23(12):100-103.
7. Chang CH, Wong KL. Printed λ/8-PIFA for Penta-Band WWAN Operation in the Mobile Phone. IEEE Transactions on Antennas and Propagation. 2009; 57(5):1373-1381.
8. Bodhaye NA and Zade PL. Design of Multi-band Double I-shaped slot Microstrip Patch Antenna With Defected Ground Structure for Wireless Application. IOSR Journal of Electronics and Communication Engineering (IOSR-JECE). 2018;13(1):25-31.
9. Dong Y, Toyao H, Itoh T. Design and characterization of miniaturized patch antennas loaded with complementary split-ring resonators. IEEE Transactions on antennas and propagation. 2011; 60(2):772-785.
10. Su SW. High-gain dual-loop antennas for MIMO access points in the 2.4/5.2/5.8 GHz bands. IEEE Transactions on Antennas and Propagation. 2010; 58(7):2412-2419.
11. Abdulhasan RA, Alias R, Ramli KN, Seman FC, Abd-Alhameed RA, Jawhar YA. Directional and isolated UWB-MIMO antenna-based uniplanar UWB-FSS array and T-strip for bi-static microwave imaging: Baggage-scanner. International Journal of RF and Microwave Computer-Aided Engineering. 2022; 32(2):e22960
12. Riaz S, Zhao X. An Eight-Port Frequency Reconfigurable MIMO Slot Antenna with Multi-Band Tuning Characteristics. In 2018 12th International Symposium on Antennas, Propagation and EM Theory (ISAPE). IEEE. 2018; 1-4. https://doi.org/10.1109/ISAPE.2018.8634212.
13. Wong KL, Lee LC. Multiband printed monopole slot antenna for WWAN operation in the laptop computer. IEEE transactions on antennas and propagation. 2009;57(2):324-330.
14. Cao Y, Yuan B, Wang G. A compact multiband open-ended slot antenna for mobile handsets. IEEE Antennas and Wireless Propagation Letters. 2011;10:911-914.
15. Lu YC, Lin YC. A mode-based design method for dual-band and self-diplexing antennas using double T-stubs loaded aperture. IEEE Transactions on Antennas and Propagation. 2012;60(12):5596-5603.
16. Chiang MJ, Wang S, Hsu CC. Compact multifrequency slot antenna design incorporating embedded arc-strip. IEEE Antennas and Wireless Propagation Letters. 2012;11:834-837.
17. Kunwar A, Gautam AK, Kanaujia BK, Rambabu K. Circularly polarized D-shaped slot antenna for wireless applications. International Journal of RF and Microwave Computer-Aided Engineering. 2019;29(1):e21498.
18. Prasad BS, Prasad MV. Design and analysis of compact periodic slot multiband antenna with defected ground structure for wireless applications. Progress In Electromagnetics Research M. 2020;93:77-87.
19. Saghati AP, Azarmanesh M, Zaker R. A novel switchable single-and multifrequency triple-slot antenna for 2.4-GHz bluetooth, 3.5-GHz WiMax, and 5.8-GHz WLAN. IEEE Antennas and Wireless Propagation Letters. 2010;9:534-537.
20. Lu JH and Huang BJ. Planar compact slot antenna with multi-band operation for IEEE 802.16 m application. IEEE Transactions on Antennas and Propagation. 2012;61(3):1411-1414.
21. Dang L, Lei ZY, Xie YJ, Ning GL, Fan J. A compact microstrip slot triple-band antenna for WLAN/WiMAX applications. IEEE Antennas and Wireless Propagation Letters. 2010; 9:1178-1181.
22. Hu W, Yin YZ, Fei P, Yang X. Compact triband square-slot antenna with symmetrical L-strips for WLAN/WiMAX applications. IEEE Antennas and Wireless Propagation Letters. 2011;10:462-465.
23. Bod M, Hassani HR, Taheri MS. Compact UWB printed slot antenna with extra bluetooth, GSM, and GPS bands. IEEE antennas and wireless propagation letters. 2012;11:531-534.
24. Prashanth CR and Naik MN. Design of Compact Multiband Annular-Ring Slot Antenna. Integrated Intelligent Computing, Communication and Security. 2019:771;281-292.
25. Jaiswal A, Sarin RK, Raj B, Sukhija S. A novel circular slotted microstrip-fed patch antenna with three triangle shape defected ground structure for multiband applications. Advanced Electromagnetics. 2018;7(3):56-63.
26. Madhav BT, Monika M, Kumar BS, Prudhvinadh B. Dual band reconfigurable compact circular slot antenna for WiMAX and X-band applications. Radioelectronics and Communications Systems. 2019;62(9):474-485.
27. Niu Z, Zhang H, Chen Q, Zhong T. A novel defect ground structure for decoupling closely spaced E-plane microstrip antenna array. International Journal of Microwave and Wireless Technologies. 2019;11(10):1069-1074.
28. Jenath Sathikbasha M, Nagarajan V. Design of multiband frequency reconfigurable antenna with defected ground structure for wireless applications.

Wireless Personal Communications. 2020;113:867-892.
29. Kulkarni J, Desai A, Sim CY. Two port CPW-fed MIMO antenna with wide bandwidth and high isolation for future wireless applications. International Journal of RF and Microwave Computer-Aided Engineering. 2021;31(8):e22700.
30. Cao YF, Cheung SW, Yuk TI. A multiband slot antenna for GPS/WiMAX/WLAN systems. IEEE Transactions on Antennas and Propagation. 2015;63(3):952-958.
31. Sah S, Tripathy MR, Mittal A. Multiband and Miniaturized dual layer Antenna incorporated with FSS and DGS. Advanced Electromagnetics. 2018;29(1):1-6
32. Sharma S, Tripathi CC, Rishi R. Impedance matching techniques for microstrip patch antenna. Indian Journal of Science and Technology. 2017;10(28):1-6.
33. Sonawane KH and Patil PS. Compact Multiband CP Filtering Antenna for Bandwidth Enhancement. International Research Journal of Multidisciplinary Scope. 2024;5(3):559-570.